J Neurophysiol 98: 1240–1252, 2007.
First published July 11, 2007; doi:10.1152/jn.00582.2007.

Directional Biases Reveal Utilization of Arm's Biomechanical Properties for Optimization of Motor Behavior

Jacob A. Goble,[1] Yanxin Zhang,[2] Yury Shimansky,[1,3] Siddharth Sharma,[2] and Natalia V. Dounskaia[1,2]
[1]*Harrington Department of Bioengineering,* [2]*Department of Kinesiology, and* [3]*Biodesign Institute, Arizona State University, Tempe, Arizona*

Submitted 23 May 2007; accepted in final form 10 July 2007

Goble J, Zhang Y, Shimansky Y, Sharma S, Dounskaia NV. Directional biases reveal utilization of arm's biomechanical properties for optimization of motor behavior. *J Neurophysiol* 98: 1240–1252, 2007. First published July 11, 2007; doi:10.1152/jn.00582.2007. Strategies used by the CNS to optimize arm movements in terms of speed, accuracy, and resistance to fatigue remain largely unknown. A hypothesis is studied that the CNS exploits biomechanical properties of multijoint limbs to increase efficiency of movement control. To test this notion, a novel free-stroke drawing task was used that instructs subjects to make straight strokes in as many different directions as possible in the horizontal plane through rotations of the elbow and shoulder joints. Despite explicit instructions to distribute strokes uniformly, subjects showed biases to move in specific directions. These biases were associated with a tendency to perform movements that included active motion at one joint and largely passive motion at the other joint, revealing a tendency to minimize intervention of muscle torque for regulation of the effect of interaction torque. Other biomechanical factors, such as inertial resistance and kinematic manipulability, were unable to adequately account for these significant biases. Also, minimizations of jerk, muscle torque change, and sum of squared muscle torque were analyzed; however, these cost functions failed to explain the observed directional biases. Collectively, these results suggest that knowledge of biomechanical cost functions regarding interaction torque (IT) regulation is available to the control system. This knowledge may be used to evaluate potential movements and to select movement of "low cost." The preference to reduce active regulation of interaction torque suggests that, in addition to muscle energy, the criterion for movement cost may include neural activity required for movement control.

INTRODUCTION

Demands of daily living promote optimization of movement characteristics, such as speed and accuracy, while minimizing effort for movement production. How this optimization is achieved has been a focus of extensive research in the area of optimal control of human movements. Various cost functions have been proposed (Todorov 2004); however, it is difficult to ascertain what is actually being optimized, as well as how this optimization process is organized. We hypothesize that the CNS exploits biomechanical properties of the limbs to increase efficiency of movement control. The study specifically focuses on biomechanical factors that influence performance of multijoint arm movements. Three such factors have been recognized: interaction torque (IT), inertial resistance, and kinematic manipulability. IT results from mechanical influence of arm segments on each other during motion (Hollerbach and Flash 1982). Inertial resistance characterizes muscle effort necessary to produce a given acceleration of the arm endpoint (Hogan 1985). Kinematic manipulability characterizes angular velocity at the joints required to produce a given endpoint velocity (Yoshikawa 1985, 1990).

To produce goal-directed movements, muscular control must be adjusted to all these factors. Each factor depends on movement direction, thus imposing differential demands for muscular control across movement directions. For instance, IT assists horizontal shoulder-elbow movements in the left-diagonal direction, i.e., when one joint flexes and the other extends. However, it resists motion in the lateral direction in which both joints simultaneously flex or extend (Dounskaia et al. 2002a; Gribble and Ostry 1999). In contrast, inertial resistance is the highest in the left-diagonal direction and the lowest in the right-diagonal direction (Gordon et al. 1994). Finally, kinematic manipulability suggests that joint rotations of the same angular amplitude would be the most efficient (in terms of the production of the highest tangential velocity) when the two joints simultaneously flex or extend, i.e., during movements approximately in the lateral direction (Dounskaia 2007).

The anisotropic properties of the biomechanical factors result in variations of the effort for movement production across directions, depending on each factor. A specific hypothesis tested here is that the CNS has knowledge of "movement cost" associated with the effect of the biomechanical factors in each movement direction and that this knowledge is used at the stage of movement planning to increase efficiency of performance by preferring movements in directions characterized by low cost and by avoiding movements in directions of high cost.

To quantify "movement cost," we formulated cost functions associated with each factor (see METHODS). The cost functions characterizing the effect of inertial resistance and kinematic manipulability across movement directions are developed with use of established mathematical descriptions of the two biomechanical factors (Hogan 1985; Yoshikawa 1985, 1990). To develop a cost function addressing the effect of IT, we exploited a recently formulated leading joint hypothesis that provides interpretation of multijoint movement control (Dounskaia 2005; Dounskaia et al. 1998, 2000a). This hypothesis suggests that during movements of the shoulder-elbow linkage, one of these joints is controlled independently of IT similar to a whip handle. Motion at this (leading) joint causes powerful IT at the other (subordinate) joint, and therefore the locus of complexity of IT regulation is at the subordinate joint. These considerations predict advantage of two movement types that allow minimal interference with the effect of IT. They emerge

Address for reprint requests and other correspondence: N. V. Dounskaia, Dept. of Kinesiology, Arizona State Univ., PO Box 870404, Tempe, AZ 85287-0404 (E-mail: Natalia.Dounskaia@asu.edu).

The costs of publication of this article were defrayed in part by the payment of page charges. The article must therefore be hereby marked "*advertisement*" in accordance with 18 U.S.C. Section 1734 solely to indicate this fact.

when the shoulder (elbow) is actively accelerated/decelerated and the elbow (shoulder) moves passively, caused by IT. Movements of these types are performed approximately in the left- and right-diagonal directions, respectively. Two cost functions optimized on these two movement types are formally developed in METHODS.

The prediction that there is a tendency to move in directions of low cost can be tested if subjects have a choice of movement direction. Traditional tasks of arm movements are not appropriate for this purpose because they restrict movement direction. For instance, reaching, pointing, and drawing tasks prescribe the initial and final point or even a specific path, and thus obligate movement in a specific direction. To provide a choice of movement direction, a novel, free-stroke drawing task modified from a task used in handwriting studies (Van Sommers 1984) is used here. Subjects were instructed to make strokes on a table surface from a circle center to the perimeter in different directions, choosing the direction in a random order. This task is advantageous because it provides a choice of movement direction for each stroke. The freedom to choose movement direction allowed subjects to display directional biases despite instructions that encouraged a uniform distribution of strokes across directions. These directional biases were compared with predictions of the formulated cost functions to distinguish factors influencing the choice of movement direction.

To provide a comprehensive analysis of factors contributing to directional biases, cost functions adopted from previous research were included in addition to the cost functions associated with the three biomechanical factors. The additional cost functions represented optimization of trajectory smoothness (Flash and Hogan 1985), muscle torque change (Uno et al. 1989), and sum of squared muscle torque (Yen and Nagurka 1988). The inclusion of these optimization criteria provided a possibility to compare the traditional and biomechanical cost functions in terms of their contribution to the emergence of directional biases. The approach of this study opens new perspectives for investigation of optimization processes underlying movement control and of how control is adapted to biomechanical properties of human limbs.

METHODS

Subjects

Fifteen students (denoted as S1–S15) from Arizona State University between 20 and 30 yr of age participated in this study after providing informed consent. Each participant was compensated with course credit for their involvement in the study. The institutional review board at Arizona State University approved the experimental protocol. All subjects were right-handed and were without any known neurological or musculoskeletal impairments.

Procedure and design

Subjects were seated at a height-adjustable table such that their right arm was parallel to the floor (shoulder abducted 90°). All movements were performed along the table's surface with the right arm in the horizontal plane using flexions/extensions of the elbow and shoulder. The upper arm segment was supported in a sling suspended from the ceiling to support the weight of the arm. Motion at the trunk was prevented by restraining the torso between the edge of the table and the back of the chair. The index finger was splinted to prevent motion relative to the hand, thus ensuring that arm movements consisted of 2 df. Finally, the index finger and splint were wrapped with Micropore paper tape (3M, St. Paul, MN) to reduce friction along the table surface, which was covered by a Plexiglas material. The task occurred within a circular workspace having a radius of 18 cm. The workspace was centered according to the position of the fingertip when the shoulder and elbow possessed joint angles of $\varphi = 30°$ and $\theta = 100°$, respectively, thus enabling a consistent starting arm posture across subjects (Fig. 1*A*). Joint angles were verified with use of the OPTOTRAK software and manual measurements with a simple goniometer. Movements from the center to the perimeter of the workspace could be performed in all directions without approaching the limits permitted by the range of motion at the joints. This measure minimized the influence of passive mechanical constraints associated with these limits for joint rotation, thus ensuring active control of joint motions throughout each stroke.

The circular workspace center was denoted by a dark circle having a diameter of 2.5 cm and overlaid with a soft fabric-like material. Movements were initiated from the center and terminated at the circle perimeter. Subjects were instructed to perform this movement with their fingertip along a straight trajectory. On reaching the workspace boundary, the subject ceased movement, lifted their fingertip from the table surface, and returned to the center to initiate a subsequent stroke. The accuracy of reaching the perimeter was not emphasized, and it was not considered during data analysis. Instead, instructions were related to production of the free-stroke drawing task. Subjects were instructed to randomly produce movements from the center to the perimeter in as many different directions as possible. Thus they were not provided any guidance as to the specific direction in which each movement should be performed. However, subjects were specifically encouraged to choose directions equally around the circle, thus emphasizing a requirement for a uniform distribution of movement directions. The freedom in the choice of movement direction provided

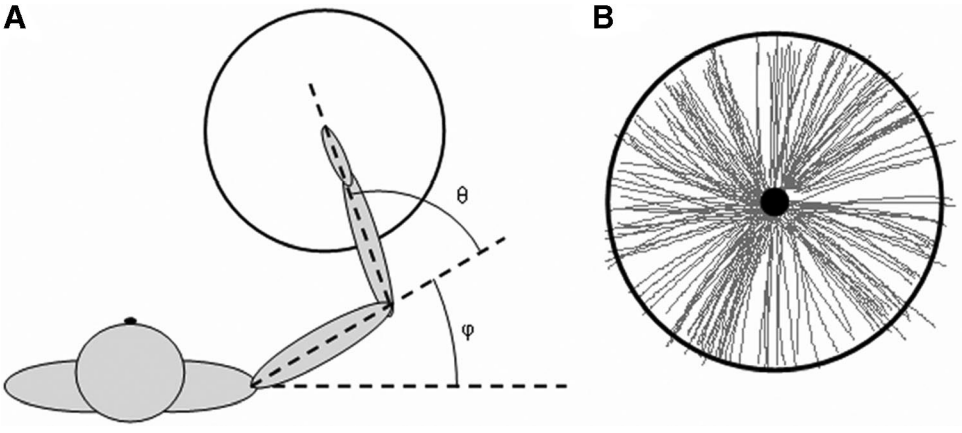

FIG. 1. Definition of workspace and joint angles. *A*: subjects were asked to produce movements within a circular workspace having a radius of 18 cm. Location of circle center was defined by shoulder and elbow joint angles of 30 and 100°, respectively. Joint angles for the elbow and shoulder are denoted by θ and φ, respectively. Positive values of θ and φ corresponded to flexion at both the elbow and shoulder joints. *B*: example of strokes produced by a representative subject (S12). Gray lines show strokes accepted for analysis.

a possibility to reveal inherent control strategies of arm movement optimization.

The task was repeated at a comfortable pace for eight 15-s trials. Several practice trials were provided to allow each subject an opportunity to familiarize themselves with the procedure. During these practice sessions, subjects were provided verbal feedback regarding whether the manner they performed strokes was consistent with the instructions. No visible trace of fingertip motion was provided to the subjects, and no comments were given regarding the order in which movement orientations should be realized. Rather, we repeatedly emphasized the instructions to randomly draw strokes in as many different directions as possible during each trial.

Apparatus and recording

Four infrared emitting diodes (IREDs) were positioned on the trunk, right shoulder, elbow, and index fingernail of each subject. Time varying position data were recorded at a sampling rate of 200 Hz using an OPTOTRAK (Northern Digital, Waterloo, Ontario, Canada) three-dimensional optoelectronic system that had been calibrated according to the manufacturer's specifications and that had accuracy of ~0.2 mm.

Data analysis

Discrete stroke segments were identified from the continuous 15 s of data collected during each trial using a series of rules. First, strokes were required to have been produced in the horizontal plane along the table surface as shown by the *z*-axis component of the fingertip marker. Second, no portion of the stroke could have a curvature value exceeding 50 m^{-1}. This threshold allows for relatively high curvature represented by 2 cm of the radius of a circle instantaneously approximating the curve of the trajectory. The curvature limitation was used to exclude instances where subjects neglected to lift their finger after a center-out movement and while bringing the finger back to the center. Curvature, *C*, was computed as

$$C = \frac{|\dot{x} \cdot \ddot{y} - \ddot{x} \cdot \dot{y}|}{(\dot{x}^2 + \dot{y}^2)^{3/2}} \quad (1)$$

where $\dot{x},\dot{y}$ and $\ddot{x},\ddot{y}$ represent the first and second derivatives of the (x,y) position data, respectively. Third, strokes were required to have been drawn in a center out fashion. This criterion was manually verified by considering the median movement initiation point as the workspace center during data processing. Strokes that were not initiated within a 4-cm radius from this point were excluded, thus ensuring that return movements were not considered in the analysis. Fourth, initial and final stroke portions during which velocity was <3% of its peak value achieved during production of this stroke were removed from the analyzed trajectories. Fifth, each stroke was required to have contained a minimum of 100 ms of data. Finally, strokes were required to have a minimum length of 12.5 cm. Figure 1*A* provides an illustrative example from S12 of a typical set of strokes accepted for analysis based on the aforementioned criteria.

Endpoint kinematics

Endpoint motion was evaluated using the position of the fingertip marker. The angular orientation of each stroke was determined with use of the line connecting the location of the endpoint at stroke initiation and termination. The orientation β_s corresponded to 0° assigned to movements to the right in the mediolateral direction, whereas 90° was associated with movements drawn away from the subject in the anterioposterior direction. This angular coordinate was used to denote stroke orientations in the extrinsic space.

The orientation data generated during each of the subjects' eight trials were combined for simultaneous analysis to depict the distribution of stroke orientations. Polar histograms of stroke orientations were produced for each subject by placing the orientation data into 72, 5° bins. These histograms were smoothed using a standard normal kernel smoothing function having a window width of 5°, yielding a probability density estimate for each orientation (Bowman and Azzalini 1997). The obtained individual histograms of stroke orientations are shown in Fig. 2 as a curve outlining the gray area in each polar plot. This representation was developed in two steps. First, the amplitude of normal kernel probability density estimate of the binned orientation data were normalized to the amplitude of a uniform distribution of stroke orientations (designated by the small black circle shown for each subject). Thus ranges in which the amplitude of the smoothed histogram exceeded 1.0 indicated a denser distribution of strokes than that of a uniform distribution. Second, for visualization purposes, this estimate was individually scaled to the peak amplitude of the signal. The value of the estimate in each direction is proportional to the probability that a subsequent stroke will be produced along that direction. It should be noted that if a linear representation of the histograms was used, the area included within the bounds of the probability density estimate would be numerically equal to the area included within the bounds of the uniform distribution circle. However, the polar representation of this data distorted the image such that these two areas do not appear equal.

In addition to building histograms for the orientations of the whole strokes, this method was also applied to the first 60 ms of stroke data to evaluate the initial trajectories of movement. In both cases, each histogram was evaluated to identify the location of statistically significant peaks and to determine the range defining the stroke clusters beneath these peaks. These significant clusters were interpreted as directional biases, and they were further examined to ascertain whether they could be accounted for by any of the tested cost functions.

Identification of significant peaks and stroke clusters

Whereas the identification of an individual peak within a unimodal distribution (e.g., Gaussian distribution) is relatively straightforward, statistical methods for the identification of multiple significant peaks within a multimodal distribution is still under development. Thus multimodal procedures often entail some subjective aspects. In an attempt to minimize this subjectivity, the mode existence test was recruited to both ascertain whether stroke orientations were uniformly distributed and to study the significance of any suspected directional biases (Minnotte 1997; Minnotte and Scott 1993). This test revealed whether a peak (suspected mode) identified in the polar histogram of orientation data at direction x was either an artifact of the sample or a true feature of the population. In short, raw orientation data were first binned and smoothed using an average shifted histogram estimator to produce the probability density estimate $f(x)$ (Minnotte 1997; Scott 1985). The shape of this estimate is dependent on the bin width, also known as the bandwidth of the kernel smoothing window h. If h is sufficiently increased, the data may be grouped under a single mode. Alternatively, as h is decreased, additional local maxima of the density estimate become apparent through a process known as splitting. Recognizing this feature of the density estimate, the value of h was decreased to the smallest value where the suspected mode at location x remained a single peak. At this bandwidth, a test statistic was calculated from the density estimate of the sample $f(x)$ according to

$$M = \int_a^b \{f(x) - \max[f(b),f(a)]\}_+ \, dx \quad (2)$$

where a and b are the adjacent local minima to the left and right of the suspected peak, respectively, and + denotes integration through only positive values of the expression within the square brackets. A new probability distribution $g(x)$ was generated whereby its value within the bounds $[a,b]$ was equal to $\max[f(b),f(a)]$. Outside the bounds $[a,b]$,

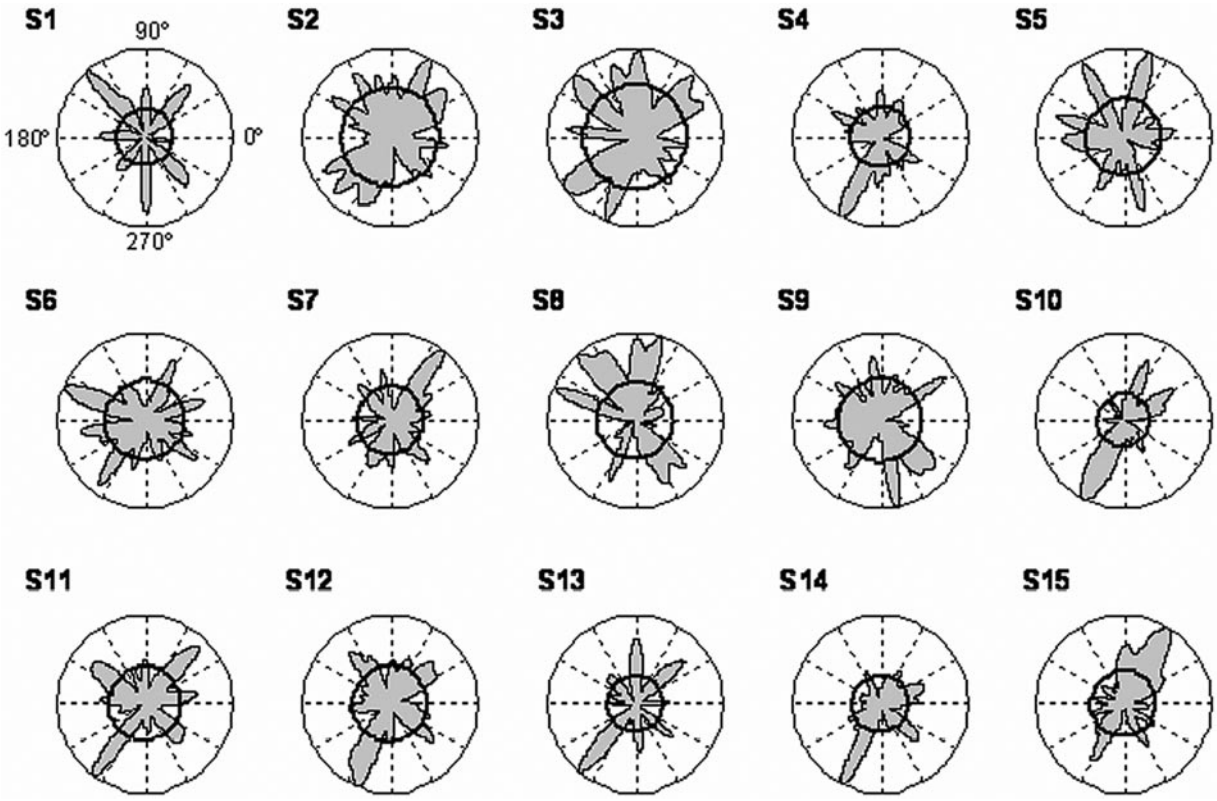

FIG. 2. Normalized smooth circular histograms showing distribution of stroke orientations for each subject. Probability densities are represented by contour of gray area. Had subjects fulfilled requirements of task to move equally across all directions, boundary of gray area would fall completely within dark circle representing uniform distribution of stroke orientations. Histogram peaks outside dark circle show that distributions were nonuniform in all subjects.

$g(x)$ was qualitatively identical to $f(x)$. A series of 400 sequential Monte Carlo data resampling procedures was performed using the probability density defined by $g(x)$, and a probability value was assigned according to the percentage of resampling procedures where the value of M from the jth resample was greater than or equal to the original M-value describing $f(x)$ (Besag and Clifford 1991; Minnotte 1997). This procedure was performed for each suspected peak to ascertain whether they were indeed statistically significant. Because of the conservative nature of tests for multimodality, peaks were considered significant at $P \leq 0.15$ (Izenman and Sommer 1988; Minnotte 1997).

The output of the mode existence test provided the direction of each peak, the bin size h at which they were deemed significant, and the range of orientations defining the corresponding cluster of strokes. Because this test identified different peaks at various levels of h, the direction of each peak and its adjacent minima differed slightly from that displayed in a graphical format. This variation was a consequence of using a constant 5° bin size for the graphical representation of the stroke distribution data. Therefore to maintain consistency in the representation of the data, the location of each peak was aligned to the position of the maximum defining the corresponding cluster of strokes in the 5° histogram. Accordingly, the boundaries of the stroke cluster were also adjusted to the locations of the two adjacent minima found within 10° limits from the originally detected cluster boundaries. Given this identification, directional biases could be evaluated to determine whether their emergence reflected an optimization of one or more cost functions. Seven cost functions described further were examined. Prior to presenting them, characteristics of joint kinematics and kinetics used for calculation of the cost functions are described.

Joint kinematic and kinetic data

Shoulder and elbow joint angles were trigonometrically computed from the IRED position data. All kinematic data were low-pass filtered at 7 Hz (4th-order Butterworth) and differentiated to yield angular velocity and angular acceleration values. Shoulder (φ) and elbow (θ) joint angles are defined in Fig. 1*A*, with positive angular velocities associated with joint flexions. Although data from the trunk IRED were not necessary for the computation of angular displacements, they were used to verify that trunk motion was minimal during arm motion. Because movements were achieved using flexions and extensions of the shoulder and elbow joints, analyses were performed on characteristics of motion at these two joints.

Torques acting at each joint were partitioned as IT, muscle torque (MT), and net torque (NT). IT represents the passive rotational effect attributed to reaction forces at the joints caused by motion of the adjacent limb segments. MT primarily represents the effect of muscle forces on joint rotation. NT reflects the net effect of IT and MT, i.e., NT = IT + MT. The influence of gravitation was not considered because arm movements were performed in the horizontal plane. Whereas NT and IT can be directly computed from kinematic data, MT is computed as the difference of NT and IT. For this reason, MT additionally includes any rotational effect induced by residual passive factors not considered in the calculation of the IT (e.g., viscoelastic properties of muscles, tendons, ligaments, or other periarticular structures at the joint). Torques were computed according to two-joint equations of motion presented by Dounskaia et al. (2002a) as torque definition II. For these calculations, anthropometric measurements including limb segment inertia, mass, and center of mass were estimated from regression equations using the height and weight of each subject (Chaffin and Andersson 1984).

Definition of cost functions

To study factors influencing the choice of movement direction, seven cost functions were analyzed to reveal their potential contribution to directional biases. Four of the cost functions quantified the

difficulty associated with the regulation of biomechanical factors, including the IT separately at the elbow and shoulder, inertial resistance, and kinematic manipulability. Additionally, three cost functions proposed by previous research were tested, including minimum jerk, minimum change of MT, and the sum of squared MT. Each cost function is described below as an optimization index ranging from 0.0 to 1.0. Values near 1.0 corresponded to the optimal value of each index.

Index of interaction torque (I_{IT}) at the shoulder and elbow

This cost function characterizes the necessity to regulate IT with muscular control to produce a goal-directed movement. It was developed based on the leading joint hypothesis that provides an interpretation of multijoint movement control (Dounskaia 2005; Dounskaia et al. 1998, 2000a). The hypothesis suggests that during movements involving motion at both the shoulder and elbow, the locus of control complexity associated with IT regulation is at the elbow and not at the shoulder. According to this hypothesis, shoulder motion is usually controlled as a single-joint motion, without consideration of IT generated by elbow movement. This is because shoulder IT is small with respect to the inertia of the upper arm. In contrast, elbow IT is high compared with inertia of the lower arm. For this reason, the goal of elbow MT is to regulate IT and to adjust elbow motion generated by IT to task requirements. IT is mutable and can be high, and therefore IT regulation may be demanding in terms of both muscle energy and neural resources. These demands vary across movement directions, being high in some directions and low in other directions (Dounskaia et al. 2002a,b; Galloway and Koshland 2002; Levin et al. 2001). This dependence on movement direction predicts that, having a choice in movement direction, subjects may exhibit a tendency to select directions that require minimal intervention of MT for elbow IT regulation, i.e., predominantly passive elbow rotation. Given that during horizontal arm movements, only MT and IT contribute in production of joint motion (NT = MT + IT, where NT is net torque), this tendency can be quantified with the following index

$$I_{\mathrm{ITE}} = \frac{1}{T_1 - T_0} \sum_{t=T_0}^{T_1} \frac{|ITE_t|}{|ITE_t| + |MTE_t|} \tag{3}$$

where *ITE* and *MTE* are the IT and MT at the elbow, and T_0 and T_1 are the beginning and end of each stroke, respectively. Movements that were achieved with high ITE relative to MTE were considered optimal.

The dynamic dominance of the shoulder that predicts the locus of IT regulation at the elbow is not observed when shoulder amplitude is substantially lower than elbow amplitude (Galloway and Koshland 2002). The LJH suggests that the two joints switch the roles during movements of this type. The elbow is rotated predominantly actively (through MT), whereas shoulder IT is influential and needs to be regulated. This predicts another possible preference in the choice of joint control (and hence, movement direction), i.e., active elbow rotation accompanied by passive shoulder motion. To test this prediction, I_{ITS} was included in the analysis. This index was computed in a similar fashion as I_{ITE} by replacing values of *ITE* and *MTE* with values of shoulder IT and MT, respectively.

Index of inertial resistance (I_{IR})

Inertial resistance characterizes the relationship between force applied at the endpoint and endpoint acceleration caused by the inertia of the arm segments. The dependence of this relationship on movement direction has been experimentally shown (Gordon et al. 1994; Mussa-Ivaldi et al. 1985) and has additionally been quantified by Hogan (1985). Specifically, the matrix T_{IR} expressing the inertial resistance experienced at the endpoint has the form

$$T_{\mathrm{IR}} = (J')^{-1} M J^{-1} \tag{4}$$

where J is the 2×2 Jacobian matrix relating joint angles to Cartesian coordinates and M reflects the 2×2 matrix of the limb's inertial properties. Both J and M were of the same form used by previous authors (Lacquaniti et al. 1993; Sabes and Jordan 1997), but were individually customized to the anthropometric properties of each subject and were computed for each stroke with use of initial joint angles. The major (minor) eigenvector of T_{IR} denotes the direction having the greatest (least) amount of inertial resistance. For the purposes of this study, the chosen index of inertial resistance (I_{IR}) was defined as

$$I_{\mathrm{IR}} = 1.0 - \frac{|\psi_s - E_{\mathrm{min,IR}}|}{\pi/2} \tag{5}$$

where ψ_s is the angular orientation of the stroke, and $E_{\mathrm{min,IR}}$ denotes the orientation of the minor eigenvector of T_{IR}. Movements oriented in the direction of least inertial resistance were considered optimal.

Index of kinematic manipulability (I_{KM})

Kinematic manipulability represents a property of the kinematic structure of the arm according to which similar angular velocities at the shoulder and elbow can realize different resultant velocities at the endpoint depending on the combination of flexion and extension at the two joints. For example, consider the case where shoulder flexion is combined with either elbow flexion or elbow extension. Let $\mathbf{V}_{\mathrm{sf}}$, $\mathbf{V}_{\mathrm{ef}}$, and $\mathbf{V}_{\mathrm{ee}}$ represent the components of endpoint velocity induced by shoulder flexion, elbow flexion, and elbow extension, respectively, and $|\mathbf{V}_{\mathrm{ef}}| = |\mathbf{V}_{\mathrm{ee}}|$. The magnitude of the resultant velocity experienced at the endpoint is greater when the two joints rotate in flexion compared with the case when the shoulder flexes and the elbow extends. The dependence of endpoint velocity on the joint coordination pattern, referred to as kinematic manipulability, has been quantified for multijoint movements of robotic systems by Yoshikawa (1985, 1990) and discussed with respect to arm movements (Dounskaia 2007; Graham et al. 2003; Sabes and Jordan 1997). The matrix of kinematic manipulability (T_{KM}) quantifying this relationship has the form

$$T_{\mathrm{KM}} = JJ' \tag{6}$$

For the two-joint system, the major (minor) eigenvectors of T_{KM} denote the directions in which maximum (minimum) endpoint velocity may be achieved. For the purposes of this study, the index of kinematic manipulability (I_{KM}) was represented as

$$I_{\mathrm{KM}} = 1.0 - \frac{|\psi_s - E_{\mathrm{maj,KM}}|}{\pi/2} \tag{7}$$

where ψ_s is the angular orientation of the stroke, and $E_{\mathrm{maj,KM}}$ denotes the orientation of the major eigenvector of T_{KM}. Movements performed in directions allowing for the maximization of kinematic manipulability (i.e., endpoint velocity) were considered optimal.

Index of minimum jerk (I_{MJ})

The minimum jerk model has offered a resilient explanation for associated characteristics of endpoint trajectory formation (Flash and Hogan 1985; Hogan 1984; Todorov and Jordan 1998). The tendency to minimize jerk is tested with the use of an index (modified from Wolpert et al. 1995)

$$I_{\mathrm{MJ}} = 1.0 - \frac{JRK_s}{\max_s(JRK_s)} \tag{8}$$

where

$$JRK_s = \frac{1}{2 \cdot L_S} \int_{T_{0_s}}^{T_{1_s}} \left[\left(\frac{d^3x}{dt^3} \right)^2 + \left(\frac{d^3y}{dt^3} \right)^2 \right] dt \quad (9)$$

Here, JRK_s represents the amount of jerk associated with stroke s normalized to its length L_s, T_0 and T_1 indicate the time of movement initiation and termination, respectively, and (x,y) indicate the instantaneous position of the endpoint. Thus I_{MJ} denotes the amount of jerk associated with each of the strokes normalized to the greatest amount of jerk observed from the set of all strokes.

Index of minimum torque change (I_{MTC})

The minimum torque change model was proposed by Uno et al. (1989). The applicability of this model for the description of directional biases was evaluated using the following index (modified from Wolpert et al. 1995)

$$I_{MTC} = 1.0 - \frac{TC_s}{\max_s (TC_s)} \quad (10)$$

where

$$TC_s = \frac{1}{2 \cdot L_s} \int_{T_{0_s}}^{T_{1_s}} \left[\left(\frac{d\,MTE}{dt} \right)^2 + \left(\frac{d\,MTS}{dt} \right)^2 \right] dt \quad (11)$$

Here, TC_s represents the amount of integrated muscle torque change associated with stroke s normalized to its length L_s, and MTE and MTS indicate the instantaneous muscle torque apparent at the elbow and shoulder, respectively. Thus I_{MTC} represents the amount of integrated muscle torque change normalized to the maximum value of TC_s, observed from the set of all strokes.

Index of minimum sum of squared torque (I_{MSST})

Optimal control modeling has often considered movement trajectories from the perspectives of a minimization of muscle energy (see Todorov 2004 for review). A simplified approach for approximating the energy expenditure is to compute the integrated sum of squared MT. Accordingly, we define the corresponding index as

$$I_{MSST} = 1.0 - \frac{MSST_s}{\max_s (MSST_s)} \quad (12)$$

where

$$MSST_s = \frac{1}{L_s} \int_{T_{0_s}}^{T_{1_s}} [MTE^2(t) + MTS^2(t)] dt \quad (13)$$

Here, $MSST_s$ denotes the integrated sum of elbow and shoulder muscle torque (MTE and MTS, respectively) for each stroke s having length L_s. Thus I_{MSST} is a simplified representation of the energetic cost associated with the production of each stroke relative to the maximum energetic cost of all strokes.

It was investigated in this study to what extent optimization of any of the listed cost functions may account for directional biases revealed with the free-stroke drawing task.

Statistical analysis

In addition to the mode existence test, statistical analyses included a repeated-measures one-way ANOVA assessing differences in the number of movements described by distinct cost functions. Pairwise comparisons were performed using Tukey's honestly significant difference (HSD) test. This method was applied where appropriate using a significance (α) level of 0.05.

RESULTS

Endpoint kinematics

Subjects produced 17.2 ± 4.6 (SD) strokes having a length of 17.4 ± 2.1 cm during each 15-s trial. The distribution of stroke orientations was first examined for each subject using a smoothed, normalized polar histogram of the fingertip marker orientation data (Fig. 2). These histograms provide the probability density for all orientations and offer a visual depiction of the subjects' tendencies to deviate from the assigned task, i.e., a uniform distribution of stroke orientations as indicated by the black circle on each plot. Apparent from a qualitative examination of Fig. 2, subjects displayed clear affinities for movements in various preferred directions. This was confirmed by the mode existence test that revealed 6.7 ± 1.7 significant histogram peaks exceeding the uniform distribution across the subjects. Table 1 summarizes the results of the mode existence test, indicating the number of significant histogram peaks that exceeded the level of uniform distribution and their respective orientations. For instance, six significant stroke clusters were distinguished in the S1 histogram. These clusters correspond to pronounced histogram peaks, revealing a preference of this subject to produce strokes of respective orientations. In contrast, movements in the directions between the distinguished peaks were consistently avoided by this subject, as suggested by low values of the histogram in these directions. Similarly, histograms of all other subjects displayed pronounced peaks exceeding the uniform distribution, confirming that all subjects had significant directional biases.

Consistency of directional biases

Although Fig. 2 and Table 1 showed that subjects did not produce a uniform distribution of stroke orientations, questions still remained regarding the consistency of the stroke orienta-

TABLE 1. *Significant histogram peaks exceeding a uniform distribution*

Subject	No. of Peaks	Orientations of Significant Histogram Peaks
S1	6	48.5°, 131.9°, 178.6°, 228.0°, 271.1°, 311.2°
S2	4	41.0°, 63.2°, 224.8°, 245.4°
S3	8	25.6°, 46.6°, 135.4°, 173.4°, 216.6°, 250.1°, 307.2°, 349.4°
S4	9	60.5°, 90.3°, 129.6°, 152.9°, 169.5°, 184.1°, 243.3°, 266.9°, 327.1°
S5	6	7.4°, 31.9°, 72.3°, 163.0°, 182.4°, 285.0°
S6	7	63.1°, 157.9°, 190.3°, 233.9°, 255.2°, 322.9°, 343.0°
S7	7	9.4°, 53.1°, 100.0°, 133.1°, 209.7°, 246.8°, 312.4°
S8	4	73.2°, 130.9°, 158.8°, 296.7°
S9	8	33.3°, 97.4°, 140.2°, 169.6°, 184.6°, 200.8°, 235.2°, 318.8°
S10	4	31.1°, 68.1°, 242.6°, 304.2°
S11	7	11.2°, 47.0°, 89.5°, 140.4°, 175.1°, 233.5°, 311.9°
S12	9	44.6°, 67.7°, 87.1°, 128.1°, 186.7°, 248.0°, 269.6°, 320.0°, 342.1°
S13	7	0.8°, 41.5°, 88.8°, 131.0°, 230.2°, 275.2°, 317.3°
S14	8	3.1°, 20.2°, 59.9°, 75.2°, 116.6°, 205.6°, 244.4°, 316.9°
S15	7	58.7°, 87.5°, 195.4°, 224.2°, 240.8°, 299.8°, 326.9°

tion distributions across subjects. Visual inspection of the histograms suggests that multiple subjects achieved directional biases along similar orientations. In particular, almost every histogram includes pronounced peaks in the right- and left-diagonal directions. For instance, subjects S4 and S10–S14 each displayed respective biases of greatest amplitude near the right-diagonal direction, i.e., 240.3 ± 6.9°. The remaining subjects also produced a histogram peak in these directions, although these peaks were not of the greatest amplitude. Similar observations can be made with respect to a common preference to produce strokes in the left-diagonal direction.

To further analyze the consistency of the directional biases across subjects, group data were used. Stroke orientations computed for all subjects were assembled to yield the polar histogram shown in Fig. 3*A*. To obtain this histogram, the method that provided the individual histograms shown in Fig. 2 was applied to the strokes produced collectively by all subjects. The resulting distribution of stroke orientations again indicated that subjects preferred to perform movements along distinct directions. Specifically, the group data represented in Fig. 3*A* indicated that subjects primarily preferred movements approximately along the 60/240 and 135/315° axis, i.e., in the two diagonal directions. This conclusion was additionally supported by the mode existence test, indicating significant histogram peaks exceeding the level of uniform distribution at 32.3, 51.8, 131.0, 241.5, and 317.9°. Movements in other directions were generally sparse, having frequency lower than that predicted by the uniform distribution. Group data thus supported the observation from Fig. 2 that there was a common tendency to deviate from a uniform distribution of stroke orientations and that the directional biases were consistent across subjects.

In addition to the representation of whole stroke orientations (Fig. 3*A*), a histogram indicating the initial stroke orientations computed over the first 60 ms was also generated for group data (Fig. 3*B*). These computations were performed to study whether the observed biases were programmed at the stage of movement planning. In this case, the biases observed in the whole strokes would also be apparent in the initial movement portions. An alternative possibility is that the biases emerged because of a lack of compensation for biomechanical factors that caused initial deviation of trajectory from the desired direction. In this case, trajectories could be corrected at the later movement stages, which would result in distinct directional histograms obtained for the whole strokes and for the initial movement portions. A comparison between Fig. 3, *A* and *B,* shows that directional biases were similar in the two histograms. This observation suggests that the directional biases emerged at the stage of movement planning as a result of minimization of certain cost functions. Contribution of the seven cost functions described in the Introduction to the revealed directional biases is examined next.

Directions of minimal cost

The seven cost functions presented in the Introduction were next evaluated to ascertain whether any of them varied across directions and whether these variations were consistent with the biases observed in the group data. Figure 4 overlays the polar histogram of group data shown in Fig. 3*A* with the values of indices denoting the amount of jerk (*A*), integrated torque change (*B*), integrated sum of squared torque (*C*), IT regulation at the elbow joint (*D*), IT regulation at the shoulder joint (*E*), inertial resistance (*F*), and kinematic manipulability (*G*) associated with each of the subjects' movements. Each optimization index could range from 0.0 to 1.0, with 1.0 being indicative of the optimal value. Notably, Fig. 4, *A–C*, suggests that the traditionally used optimal control criteria (i.e., minimum jerk, minimum integrated torque change, and minimum sum of squared torque, respectively) realized similar values regardless of movement direction. There was no evidence that the behavior of these cost functions were directionally dependent. Moreover, values of these cost functions were not necessarily close to 1.0, suggesting that none of these functions was optimized during stroke production. Thus the three criteria do not offer any explanation why subjects preferred movements in certain directions more than others.

In contrast, Fig. 4, *D–G*, revealed that the biomechanically relevant cost functions relating to elbow and shoulder IT regulation, inertial resistance, and kinematic manipulability, respectively, displayed anisotropic behavior in which they were optimized along specific movement directions. Stroke values computed from these cost functions provided two petal-like regions in which optimal values resided ~180° apart from one another. Specifically, optimal values were noted approximately along the 120/300° axis for I_{ITE}, 45/135° for I_{ITS}, 30/210° for I_{IR}, and 15/195° for I_{KM}. This feature of directionality was absent from the traditional cost functions. For this reason, these four biomechanically relevant cost functions

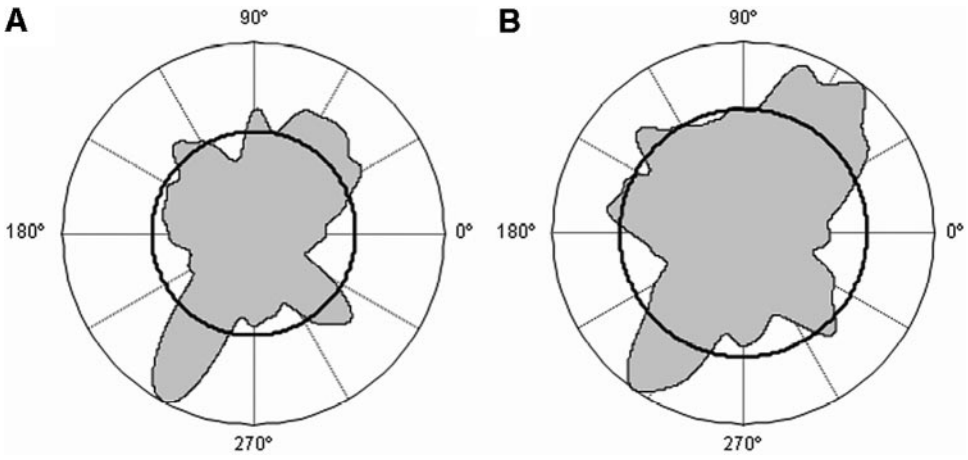

FIG. 3. Normalized smooth polar histogram showing distribution of stroke orientations for all subjects. Grouped distribution of stroke orientations indicated that subjects preferred to primarily distribute their movements along 2 axes: 60/240 and 135/315°. Uniform distribution level is noted by black circle. *A*: distributions are represented for entire stroke lengths. *B*: distributions are represented for initial portion of movement, i.e., 1st 60 ms.

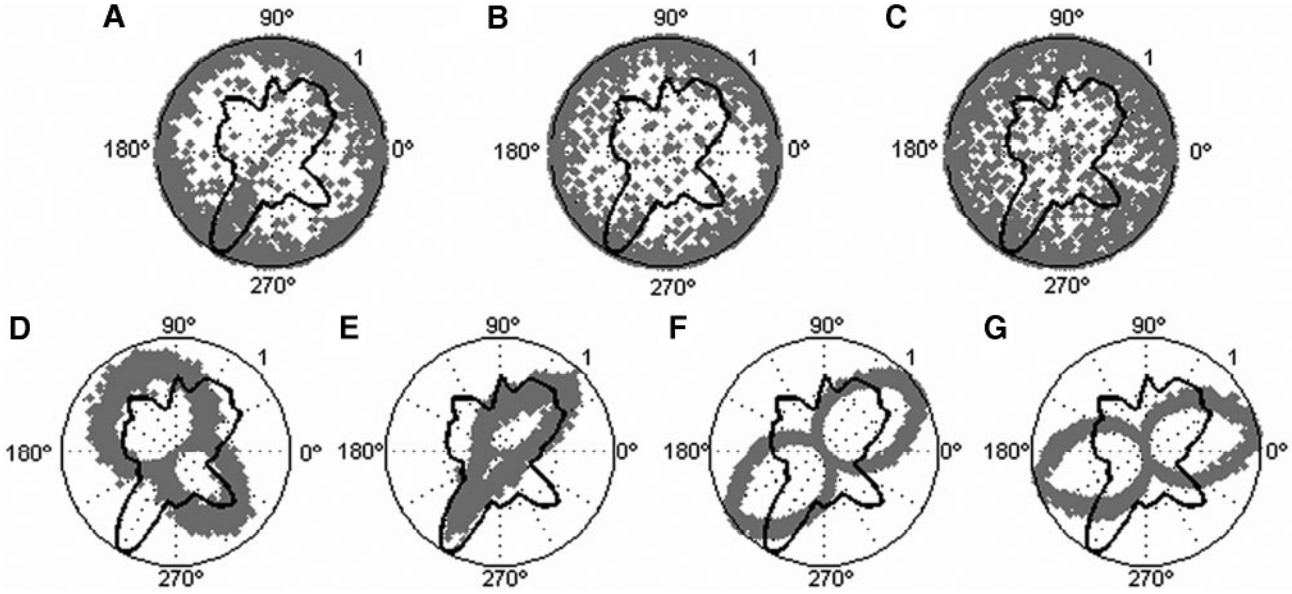

FIG. 4. Associated cost of movement from tested cost functions. Distribution of group stroke orientation data (black line) from Fig. 3*A* was overlaid with dots representing values of index of (*A*) minimum jerk; (*B*) minimum torque change; (*C*) minimum sum of squared torque; (*D*) elbow interaction torque (IT) regulation; (*E*) shoulder IT regulation; (*F*) inertial resistance; and (*G*) kinematic manipulability. Values were computed for each stroke. Values near 1.0 reflect an optimization of each index.

were studied as potential candidates for the emergence of directional biases across individual subjects. The possible explanation of individual histogram peaks by these factors was examined next.

Assessment of individual data

Figure 5 displays the histograms of individual subject stroke orientations (as displayed in Fig. 2) overlaid with traces describing the distribution of strokes optimized according to I_{ITE} (blue), I_{ITS} (red), I_{IR} (green), and I_{KM} (yellow). The uniform distribution level is noted by the black circle. In developing this figure, a stroke was considered quasi-optimal according to inertial resistance or kinematic manipulability if the respective index, I_{IR} or I_{KM}, was >0.875. Choice of this threshold was rather conservative because it included only one eighth of the possible values for each index. Additionally, strokes were considered quasi-optimal according to the criterion of elbow or shoulder IT regulation if I_{ITE} or I_{ITS} was >0.5. This threshold allowed the identification of strokes whereby $|IT|$ on average exceeded $|MT|$, suggesting that IT served as the primary source of motion at the joint.

Comparing individual stroke orientations to the group data displayed in Fig. 3*A*, each subject exhibited one or more significant histogram peaks extending beyond the level of uniform distribution along directions similar to those identified in the analysis of group data (i.e., the two diagonal directions).

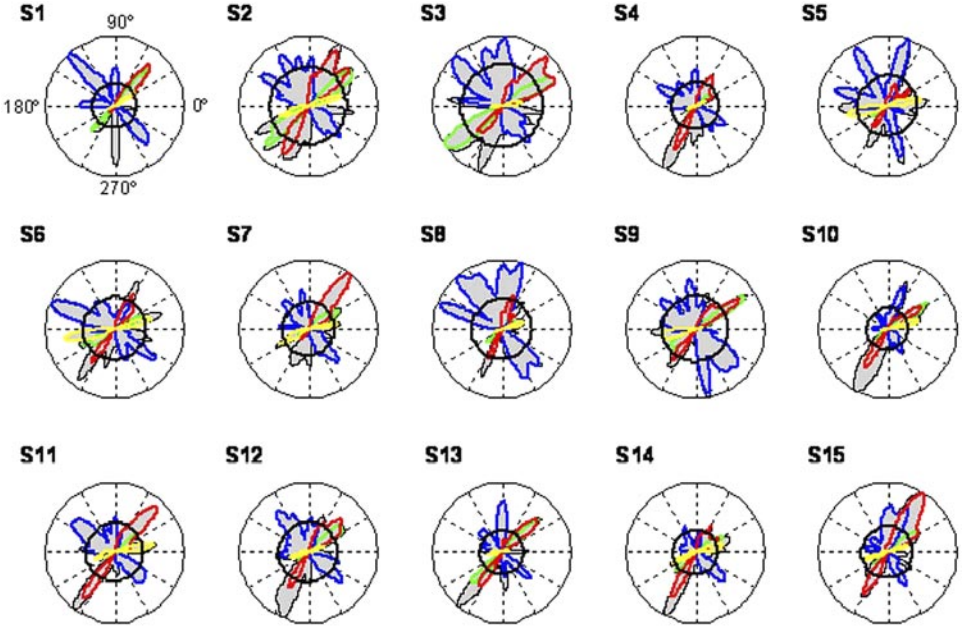

FIG. 5. Individual histograms of stroke orientations from Fig. 2 (gray area) overlaid with distributions of quasi-optimal strokes. Color traces represent strokes accounted for by optimization of I_{ITE} (blue), I_{ITS} (red), I_{IR} (green), and I_{KM} (yellow). Majority of peaks were accounted by at least 1 of 4 cost functions, suggesting that biomechanical factors provided interpretations to dominant portion of observed biases. Major peaks were accounted primarily with I_{ITE} and I_{ITS}.

Additionally, the individual data displayed in Fig. 5 indicates that a large portion of the strokes making up these histogram peaks were described by quasi-optimal values of one or more biomechanically relevant cost functions. This implies that the biomechanical factors were sufficient to account for the dominant portion of the observed biases, suggesting that no other factors may have contributed to the biases.

The next step of the analysis included a comparison across the four cost functions in terms of the contribution of each of them to the directional biases. With this purpose, contribution of each biomechanical factor to the peaks of the individual histograms was quantitatively assessed with a measure of factor contribution (*FC*). FC was defined as the percentage of the strokes belonging to a particular individual histogram peak that could be accounted for by a given cost function. Specifically, FC was computed for each peak as

$$FC = \max_{i=1,\ldots,3} \left(\frac{A_i \cap B_i}{A_i} \right) \quad (14)$$

where A_i is the area beneath a significant histogram peak *i,* and B_i is the area beneath the probability distribution of stroke orientations optimized according to one of the aforementioned cost functions and comprised within peak *i*. The FC measure was computed for each biomechanical factor. The data were analyzed only for the three major histogram peaks (in terms of peak amplitude) for each subject. The purpose of this analysis was to determine the degree to which every biomechanical factor could account for at least one of the three major peaks across subjects.

Maximum FC values resulting from the analysis of each subject's top three significant histogram peaks are provided in Table 2 for each biomechanical factor. In the majority of subjects, at least one of the three major peaks was accurately predicted by I_{ITE}. Indeed, the blue traces of Fig. 5 (i.e., the distribution of strokes optimized according to I_{ITE}) were often aligned with the exterior trace denoting the histogram peaks. FC values reflected this alignment by showing that the optimization of I_{ITE} accounted for 93.8 ± 19.6% of at least one of the top three histogram peaks. The high accuracy of the bias prediction suggests that the cost of regulating IT at the elbow joint was an influential contributor to these biases. Similarly, movements characterized by quasi-optimal values of I_{ITS} accounted for large portions of other significant histogram peaks. FC values confirmed this assessment by indicating that movements consisting of at least one of the top three significant histogram peaks were, on average, 74.5 ± 23.6% accounted for by the optimization of I_{ITS}. It should be noted that the optimization of I_{ITE} and I_{ITS} occurred in distinct directions, as indicated by the minor of overlap of the red and blue traces within the significant histogram peaks shown in Fig. 5. Accordingly, the analysis of FC revealed that at least two of the three significant histogram peaks were accounted by biomechanical factors associated with IT regulation across subjects

TABLE 2. *FC values for factors ITE, ITS, KM, and IR*

Subject	FC_{ITE}	FC_{ITS}	FC_{KM}	FC_{IR}
S1	100.0%	93.3%	26.7%	60.0%
S2	25.0%	91.7%	44.4%	77.8%
S3	100.0%	29.4%	0.0%	82.4%
S4	100.0%	48.4%	0.0%	12.9%
S5	100.0%	38.1%	0.0%	0.0%
S6	100.0%	78.6%	0.0%	25.0%
S7	100.0%	95.5%	0.0%	36.4%
S8	100.0%	43.5%	0.0%	8.7%
S9	100.0%	76.9%	7.7%	76.9%
S10	81.3%	81.8%	4.6%	95.5%
S11	100.0%	100.0%	0.0%	23.3%
S12	100.0%	100.0%	0.0%	57.1%
S13	100.0%	87.5%	4.2%	66.7%
S14	100.0%	68.0%	32.0%	68.0%
S15	100.0%	85.4%	9.8%	26.8%

With few exceptions, inertial resistance and kinematic manipulability did not account for a dominant portion of any of the top three peaks. When all significant histogram peaks were included in the analysis, it was found that the optimization of I_{IR} accounted for, on average, a 47.8 ± 0.4% factor contribution of the significant peaks. I_{KM} yielded only a 8.6 ± 14.1% factor contribution of the significant peaks. Thus the preference to minimize the regulation of either elbow or shoulder IT was stronger than the preference to optimize either inertial resistance or kinematic manipulability. This conclusion is further supported by a one-way ANOVA and pairwise comparisons indicating that the number of strokes possessing quasi-optimal values of I_{ITE} was significantly greater than those explained by all other factors ($P < 0.001$). Additionally, the number of strokes accounted for by the optimization of I_{ITS} was significantly greater than those optimized by either I_{IR} or I_{KM} ($P < 0.01$).

Assessment of unpreferred movement directions

The foregoing analyses focused on the identification of preferred movement directions and whether various biomechanical factors may have influenced their emergence. Optimization of IT contribution to NT at either the elbow or shoulder joint was identified as the most prominent biomechanical characteristic associated with the observed directional biases. To further study the role of this factor in the choice of movement direction, we study whether directions in which the IT contribution was optimized in neither of the two joints were consistently avoided. With this purpose, an analysis of unpreferred movement directions was performed. Specifically, a probability distribution $h(x)$ of unpreferred directions was assessed from the function $f(x)$ representing the group histogram of stroke orientations shown in Fig. 3*A*. The distribution $h(x)$ was defined as

$$h(x) = \begin{cases} 1 - f(x) & \text{if } f(x) \le 1 \\ 0 & \text{if } f(x) > 1 \end{cases} \quad (15)$$

Amplitude of his distribution increases in directions in which movements were unpreferred, i.e., in which $f(x) < 1$, where 1 represents the uniform distribution of stroke orientations. The distribution $h(x)$, normalized to its maximum, is shown in Fig. 6 with the gray area. Primarily these unpreferred directions resided along four orientations, as noted by peaks at 339.6, 195.1, 101.9, and 283.9°. In addition, the figure includes the optimization index values for both I_{ITE} (blue) and I_{ITS} (red) shown previously in gray color in Fig. 4, *D* and *E*, respectively. Optimization index values of 1.0 correspond to the exterior circle of Fig. 6, whereas the black circle denotes a value of 0.5 that was the threshold for the two IT-related indices. Evident from the figure, regions in which both cost functions yielded subthreshold values corresponded to the two least preferred

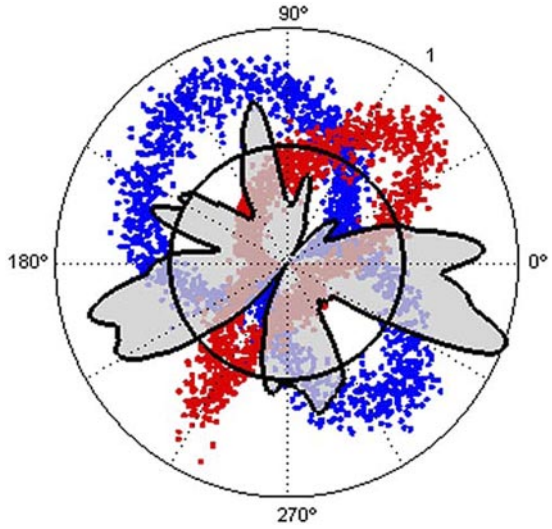

FIG. 6. Distribution of unpreferred movement directions and IT cost function values. Gray area shows distribution of unpreferred movement directions. Red and blue dots denote values of I_{ITS} and I_{ITE}, respectively. Black circle indicated threshold value (0.5) for the 2 indices. Major peaks of unpreferred movement distribution (i.e., in 195.1, 283.9, and 339.6° directions) were characterized by subthreshold or near-threshold values (residing near or within the black circle) of both indices. This result confirms that preferred directions were characterized by movements performed by active rotation at 1 joint and largely passive motion at the other joint.

movement directions, 339.6 and 195.1°. Additionally, the unpreferred movements in the 283.9° direction were characterized by strokes possessing subthreshold I_{ITS} values and I_{ITE} values that were near the threshold. Thus unpreferred movement directions often required a form of control in which MT served as an important source of motion for both joints. The overlapping of the I_{ITS} and I_{ITE} values also makes it apparent that preferred directions, i.e., the directions between the adjacent peaks of the distribution $h(x)$, were usually the directions in which one index was high and the other was low. These combinations of values of the two indices corresponds to movements performed predominantly actively (by MT) at one joint and primarily passively (by IT) at the other joint.

DISCUSSION

Although the task required movements to be produced in as many different directions as possible, subjects consistently showed directional preferences (Fig. 2). Distributions of stroke orientations were found to maintain a reasonable degree of consistency as identified by significant peak locations in both individual histograms across subjects and in the group data. Specifically, subjects primarily preferred to perform movement in the two diagonal directions, i.e., approximately along the 60/240 and 135/315° axis. The observed biases in movement direction support our hypothesis that the choice of movement direction is influenced by the knowledge of movement cost associated with some mutual set of factors.

Seven cost functions were examined as potential candidate factors. The optimization of jerk, torque change, and sum of squared torque offered a generalized description of all strokes. Regardless of the movement direction, each of these cost functions acquired similar values, revealing isotropic behavior. Moreover, values of each factor were spread between 0 and 1, indicating that the three cost functions were not optimized during stroke production. For these reasons, none of these traditionally considered cost functions could be used for explaining the emergence of preferred movement directions. In contrast, the four cost functions related to the biomechanical factors showed anisotropic behavior. Each of these functions acquired high values in some specific directions and low values in other directions. Based on these observations, the subsequent analyses were focused on the four biomechanical cost functions and their possible contribution to the directional biases.

Superimposing the values of each cost function on the directional group histogram (Fig. 4) suggested that the best prediction of the directional biases was provided by the two IT-related cost functions. Analysis of peaks in the individual histograms confirmed that these two cost functions accounted for the dominant portion of the observed biases. The dominant role of the two IT-related cost functions in production of directional biases was further supported by the analysis of unpreferred movement directions. Neither I_{ITE} nor I_{ITS} acquired quasi-optimal (close to 1.0) values during movements in these directions. These results suggest that the major directional biases emerged because of a tendency to perform two types of shoulder and elbow movements. Strokes that optimized I_{ITE} were produced with active rotation at the shoulder and predominantly passive motion at the elbow driven by IT generated by the shoulder motion. Conversely, strokes optimal in terms of I_{ITS} were executed with active rotation at the elbow and largely passive motion at the shoulder.

In addition to I_{ITE} and I_{ITS}, indices describing the associated inertial resistance and kinematic manipulability were studied. Figure 5 indicates the possible influence of these factors on the selection of movement direction. For instance, subjects S2 and S3 each displayed histogram peaks that were largely accounted by strokes possessing quasi-optimal values of I_{IR}. However, optimization of I_{IR} and I_{KM} failed to consistently account for a large proportion of the strokes contained within the top three significant histogram peaks across subjects. These results suggest that, although the influence of inertial resistance and kinematic manipulability on directional biases cannot be immediately ruled out, these effects were minor.

The possibility that biomechanical factors influence movement direction has been previously discussed in studies that reported consistent deviations of movement trajectory from a prescribed path (Dounskaia et al. 2000b, 2002b; Ketcham et al. 2004; Pfann et al. 2002). In particular, contribution of IT and inertial resistance to the observed deviations has been hypothesized. Our results support that hypothesis. Furthermore, testing cost functions associated with potential factors undertaken in this study provided assessments of contribution of each factor to the observed biases, suggesting that the dominant factor influencing directional biases is IT.

The major bias toward the minimization of muscular interference with the IT effect was predicted by the leading joint hypothesis (LJH) (Dounskaia 2005; Dounskaia et al. 2000a). The LJH suggests that the biomechanical properties of the multijoint structure of the arm, and specifically IT emerging at the joints caused by motion of adjacent joints, are exploited to organize arm movements. In this way, leading joint motion imposes large IT at the subordinate joint, and thus creates a dynamic foundation for motion of the entire limb. Accordingly,

the role of the subordinate joint's MT is to regulate the effect of IT and to adjust joint motion to the task requirements. Because of the bigger musculature and inertia of the proximal limb segment compared with the distal segment, movements in the majority of directions are shoulder-led. However, a sector of the right-diagonal directions is elbow-led because shoulder amplitude is small, and therefore the shoulder cannot be used as a motion generator in these directions. Whether shoulder- or elbow-led movements are considered, this interpretation of multijoint movement control predicts the preference to minimize effort for the regulation of the IT effect on the subordinate joint motion. Indeed, this regulation may be complex because it may require high levels of MT, fast changes in this torque, and extensive processing of sensory feedback. These considerations predict preferences to perform two types of movements. One type belongs to the category of shoulder-led movements and consists in active rotation at the shoulder and passive motion at the elbow. The other type is an elbow-led movement characterized by minimal muscle effort for regulation of passive shoulder motion. The results of this study are consistent with this prediction, thus providing support to the interpretation of the control strategy offered by the LJH.

The revealed tendency to move one joint largely passively may be interpreted as a minimization of metabolic energy expenditure. However, one of the two preferred movement directions, namely the left-diagonal direction, is one of the most demanding in terms of the required muscle force because this direction is characterized by maximal inertial resistance (Gordon et al. 1994). A possible alternative interpretation of our results is a tendency to simplify parameters of neural control not directly related to metabolic cost or mechanical load (Prilutsky and Zatsiorsky 2002). For instance, IT regulation at the subordinate joint requires intense neural feedforward computations and processing of sensory information (Dounskaia 2005). Thus the strategy to allow IT to predominantly drive subordinate joint motion may reflect a tendency to minimize energy associated with neural processing required for IT regulation by MT.

The biomechanical factors reliably accounted for major portions of the significant histogram peaks, suggesting that no other factors may have provided an important contribution to the directional biases. Nevertheless, it is possible that there were other influential factors, the effect of which may have been aligned with the effect of the tested factors. Also, there were peaks in some of the individual histograms that were not explained with any of the tested cost functions. For instance, Fig. 5 indicates that several subjects exhibited various histogram peaks along orientations that could not be fully explained (e.g., 270° peak of S1, 250° peak of S2, 240° peak of S3, etc.), suggesting a possibility of additional factors influencing the choice of movement direction. One possibility is that biases were influenced by the perceptual distinctiveness of movements in different directions. Our task limited this factor's potential influence, however, by not supplying subjects with a visual trace of their movements (Meulenbroek and Thomassen 1992). Moreover, movements in perceptually relevant orientations (i.e., vertical, horizontal, diagonal) did not seem to be a pronounced feature of individual stroke distributions (Fig. 2). Nevertheless, the role of sensory information in the emergence of the directional biases is an important question that needs to be addressed in future studies.

Another noteworthy factor is that humans are notoriously known to be bad random generators (Lopes 1982), and this characteristic may have contributed to inability of each particular subject to uniformly distribute movements. However, it is unlikely that this factor would lead to the emergence of consistent directional biases across subjects. Additionally, certain movement directions may be more favorable in terms of the associated muscle contractile dynamics, i.e., preferred movements may be in directions where the force-generating properties of the muscles are the most advantageous. The potential influence of this factor on the revealed directional biases cannot be excluded and needs to be studied with use of arm models including characteristics of muscle biomechanics.

The obtained results cast light on the organization of the optimization processes. Frequent movements in the directions of low biomechanical cost suggest that information about the limb's biomechanical structure and the way it influences movement cost is available before motion initiation. This feedforward information may be used to select movement directions of low cost. The idea that this information is available at the stage of movement planning is further supported by the finding that the directional biases were similar regardless of whether the whole movement or only the initial portion (i.e., 1st 60 ms) of this movement was considered. Indeed, the two histograms in Fig. 3 would be different if movements deviated from the chosen directions during the course of motion caused by the biomechanical factors. Movement cost might be determined from an internal model of limb biomechanics. An alternative possibility is that the knowledge of movement cost is acquired during motor learning and stored in the form of an internal model of optimal cost (Shimansky et al. 2004). As suggested in that study, the internal model of optimal cost might be a critical functional component of a neural control system capable of self-optimization. In particular, a combination of the internal model of the limb's biomechanical properties and the internal model of optimal cost would allow the CNS to optimize movement planning. Findings of this study indicate that one of the crucial determinants of movement cost is associated with the demands for regulation of the IT effect at the subordinate joint.

The dominant role of the biomechanical cost functions in the optimization of motor performance is consistent with findings of directional preferences during handwriting movements. For instance, in a study by Van Sommers (1984), subjects were given a blank sheet of paper and asked to cover it with short lines with an emphasized instruction to draw in every possible direction. Consistent biases in the orientation of the produced lines were revealed. Other studies reported deviations of movement path toward production of right-tilted strokes and ovals (Dounskaia et al. 2000b; Meulenbroek and Thomassen 1991). The observed movement preferences were interpreted as resulting from biomechanical interaction between wrist and finger movements. This interaction can either facilitate or hinder hand movements, depending on the coordination pattern between the wrist and fingers. The similarity of the preferred strokes and the ovals with the shapes of cursive letters suggested that the motor act of handwriting has been developed with observations of these biomechanical constraints of the hand to allow fast and accurate performance for a long time without fatigue.

Although this approach has suggested an important role of biomechanical factors in the organization of handwriting movements, thorough study of this phenomenon was not performed because of the complexity of the biomechanical structure of the hand. Here, we addressed the role of biomechanical factors in directional preferences by taking advantage of horizontal shoulder-elbow movements for which dynamic models have been developed and widely used (Dounskaia et al. 2002a; Hoy and Zernicke 1985; Putnam 1993; Schneider et al. 1989) and influential biomechanical factors have been extensively explored (Graham et al. 2003; Hogan 1985; Hollerbach and Flash 1982). The obtained results support the notion that biomechanical factors, and specifically IT, influence organization of multijoint movements. Furthermore, they suggest that the CNS may exploit biomechanical properties of the limbs to increase efficiency of motor performance.

The revealing of the directional biases and the cost functions underlying them may have important practical applications. Many types of daily motor activities require a sequence of arm movements in various directions. These tasks usually allow for substantial freedom in the choice of movement direction because the position of the trunk in the working environment can be changed to provide a desired movement direction for the arm. Arrangement of objects in the working space can also be adjusted to facilitate motor performance. The findings presented here open perspectives for optimization of these types of activities in terms of improvements in the efficiency of performance and of fatigue minimization.

Application of these findings to practical tasks should be derived with caution because tested movements were limited to the horizontal plane and to rotation of only two joints, the shoulder and elbow. Also, movements were equidistant and they were initiated from a single arm posture. Removing any of these restrictions may result in modifications of the preferred movement directions and of the strength of biases associated with each particular cost function. Nevertheless, it can be expected that the existence of the directional biases and the association of them with the tendency to move the subordinate joints largely passively is a robust characteristic of multijoint movements. This follows from a consideration that these directional biases were predicted by the LJH and that the leading-subordinate organization of control has been observed in various multijoint movements and not only in those restricted to shoulder and elbow rotations in the horizontal plain (Dounskaia et al. 1998; Galloway and Koshland 2002; Galloway et al. 2004; Hirashima et al. 2003, 2007). This predicts that directional biases caused by the tendency to minimize active regulation of IT would be observed in a wide range of unconstrained multijoint movements.

In conclusion, when given a choice, subjects displayed a tendency to move in specific directions. Two biomechanical cost functions associated with demands for regulation of the IT effect with MT at the shoulder and elbow were identified as primary contributors to the revealed directional biases. Significant biases predominantly corresponded to the tendency to propel one joint (either the shoulder or the elbow) passively with IT generated by motion from the adjacent joint. These biases were predicted by the LJH, and therefore they provide support for this hypothesis. Tendencies to move in directions of low inertial resistance and high kinematic manipulability were also observed, but these movements were of minor preference. The crucial contribution of the cost functions associated with regulation of the IT effect on joint motions supports the hypothesis that biomechanical properties of the limbs are exploited to increase movement efficiency. The results allow for the association of movement efficiency with metabolic energy minimization but also offer a novel optimization criterion related to minimization of neural processing required for regulation of IT during multijoint movements. The results advance research of optimal control strategies underlying human movements, revealing the important role of biomechanical factors in movement optimization. This knowledge opens new perspectives in the area of ergonomic design and research concerning the organization of everyday tasks often requiring the performance of serial reaching movements in different directions.

GRANTS

This research was supported by National Institute of Neurological Disorders and Stroke Grant NS-43502. Additionally, J. Goble was supported by a fellowship from the National Science Foundation (NSF) Integrative Graduate Education and Research Traineeship (IGERT) program on Neural and Musculoskeletal Adaptations in Form and Function (NSF 9987619).

REFERENCES

Besag J, Clifford P. Sequential Monte Carlo p-values. *Biometrika* 78: 301–304, 1991.

Bowman AW, Azzalini A. *Applied Smoothing Techniques for Data Analysis: The Kernel Approach with S-Plus Illustrations.* Oxford, UK: Clarendon, 1997.

Chaffin DB, Andersson GBJ. *Occupational Biomechanics.* New York: John Wiley, 1984.

Dounskaia N. The internal model and the leading joint hypothesis: implications for control of multi-joint movements. *Exp Brain Res* 166: 1–16, 2005.

Dounskaia N. Kinematic invariants during cyclical arm movements. *Biol Cybern* 96: 147–163, 2007.

Dounskaia N, Ketcham CJ, Stelmach GE. Commonalities and differences in control of various drawing movements. *Exp Brain Res* 146: 11–25, 2002a.

Dounskaia N, Swinnen SP, Walter CB. A principle of control of rapid multijoint movements: the leading joint hypothesis. In: *Biomechanics and Neural Control of Movement*, edited by Winter JM and Crago PE. New York: Springer-Verlag, 2000a, p. 390–403.

Dounskaia NV, Ketcham CJ, Stelmach GE. Influence of biomechanical constraints on horizontal arm movements. *Motor Control* 6: 366–387, 2002b.

Dounskaia NV, Swinnen SP, Walter CB, Spaepen AJ, Verschueren SMP. Hierarchical control of different elbow-wrist coordination patterns. *Exp Brain Res* 121: 239–254, 1998.

Dounskaia NV, Van Gemmert AWA, Stelmach GE. Interjoint coordination during handwriting-like movements. *Exp Brain Res* 135: 127–140, 2000b.

Flash T, Hogan N. The coordination of arm movements: an experimentally confirmed mathematical model. *J Neurosci* 5: 1688–1703, 1985.

Galloway JC, Bhat A, Heathcock JC, Manal K. Shoulder and elbow joint power differ as a general feature of vertical arm movements. *Exp Brain Res* 157: 391–396, 2004.

Galloway JC, Koshland GF. General coordination of shoulder, elbow and wrist dynamics during multijoint arm movements. *Exp Brain Res* 142: 163–180, 2002.

Gordon J, Ghilardi MF, Cooper SE, Ghez C. Accuracy of planar reaching movements. II. Systematic extent errors resulting from inertial anisotropy. *Exp Brain Res* 99: 112–130, 1994.

Graham KM, Moore KD, Cabel WD, Gribble PL, Cisek P, Scott SH. Kinematics and kinetics of multijoint reaching in nonhuman primates. *J Neurophysiol* 89: 2667–2677, 2003.

Gribble PL, Ostry DJ. Compensation for interaction torques during single- and multijoint limb movement. *J Neurophysiol* 82: 2310–2326, 1999.

Hirashima M, Kudo K, Ohtsuki T. Utilization and compensation of interaction torques during ball-throwing movements. *J Neurophysiol* 89: 1784–1796, 2003.

Hirashima M, Kudo K, Watarai K, Ohtsuki T. Control of 3D limb dynamics in unconstrained overarm throws of different speeds performed by skilled baseball players. *J Neurophysiol* 89: 1784–1796, 2007.

Hogan N. An organizing principle for a class of voluntary movements. *J Neurosci* 4: 2745–2754, 1984.

Hogan N. The mechanics of multi-joint posture and movement control. *Biol Cybern* 52: 315–331, 1985.

Hollerbach JM, Flash T. Dynamic interactions between limb segments during planar arm movement. *Biol Cybern* 44: 67–77, 1982.

Hoy MG, Zernicke RF. Modulation of limb dynamics in the swing phase of locomotion. *J Biomech* 18: 49–60, 1985.

Huffenus AF, Amarintini D, Forestier N. Effects of distal and proximal arm muscles fatigue on multi-joint movement organization. *Exp Brain Res* 170: 436–447, 2006.

Izenman AJ, Sommer C. Philatelic mixtures and multimodal densities. *J Am Statist Assoc* 83: 941–953, 1988.

Ketcham CJ, Dounskaia N, Stelmach GE. Age-related differences in the control of multijoint movements. *Motor Control* 8: 422–436, 2004.

Lacquaniti F, Carrozzo M, Borghese NA. Time-varying mechanical behavior of multijointed arm in man. *J Neurophysiol* 69: 1443–1464, 1993.

Levin O, Ouamer M, Steyvers M, Swinnen SP. Directional tuning effects during cyclical two-joint arm movements in the horizontal plane. *Exp Brain Res* 141: 471–484, 2001.

Lopes L. Doing the impossible: a note on induction and the experience of randomness. *J Exp Psychol Learn Mem Cogn* 8: 626–636, 1982.

Meulenbroek RGJ, Thomassen AJWM. Stroke-direction preferences in drawing and handwriting. *Hum Mov Sci* 10: 247–270, 1991.

Meulenbroek RGJ, Thomassen JWM. Effects of handedness and arm position on stroke-direction preferences in drawing. *Psychol Res* 54: 194–201, 1992.

Minnotte MC. Nonparametric testing of the existence of modes. *Ann Statist* 25: 1646–1660, 1997.

Minnotte MC, Scott DW. The mode tree: a tool for visualization of nonparametric density features. *J Comput Graph Statist* 2: 51–68, 1993.

Mussa-Ivaldi FA, Hogan N, Bizzi E. Neural, mechanical, and geometrical factors subserving arm posture in human. *J Neurosci* 5: 2732–2743, 1985.

Pfann KD, Corcos DM, Moore CG, Hasan Z. Circle-drawing movements at different speeds: role of inertial anisotropy. *J Neurophysiol* 88: 2399–2407, 2002.

Prilutsky BI, Zatsiorsky VM. Optimization-based models of muscle coordination. *Exerc Sport Sci Rev* 30: 32–38, 2002.

Putnam CA. Sequential motions of body segments in striking and throwing skills: descriptions and explanations. *J Biomech* 26: 125–135, 1993.

Sabes PN, Jordan MI. Obstacle avoidance and a perturbation sensitivity model for motor planning. *J Neurosci* 17: 7119–7128, 1997.

Schneider K, Zernicke RF, Schmidt RA, Hart TJ. Changes in limb dynamics during the practice of arm movements. *J Biomech* 22: 805–817, 1989.

Scott DW. Average shifted histograms: effective nonparametric density estimators in several dimensions. *Ann Statist* 13: 1025–1040, 1985.

Shimansky YP, Kang T, He J. A novel model of motor learning capable of developing an optimal movement control law online from scratch. *Biol Cybern* 90: 133–145, 2004.

Todorov E. Optimality principles in sensorimotor control. *Nat Neurosci* 7: 907–915, 2004.

Todorov E, Jordan MI. Smoothness maximization along a predefined path accurately predicts the speed profiles of complex arm movements. *J Neurophysiol* 80: 696–714, 1998.

Uno Y, Kawato M, Suzuki R. Formation and control of optimal trajectory in human multijoint arm movement: minimum torque-change model. *Biol Cybern* 61: 89–101, 1989.

Van Sommers P. *Drawing and Cognition.* Cambridge, MA: Cambridge University Press, 1984.

Wolpert DM, Ghahramani Z, Jordan MI. Are arm trajectories planned in kinematic or dynamic coordinates? An adaptation study. *Exp Brain Res* 103: 460–470, 1995.

Yen V, Nagurka ML. A suboptimal trajectory planning algorithm for robotic manipulators. *ISA Trans* 27: 51–59, 1988.

Yoshikawa T. Manipulability of robotic mechanisms. *Int J Robot Res* 4: 3–9, 1985.

Yoshikawa T. *Foundations of Robotics: Analysis and Control.* Cambridge, MA: MIT Press, 1990.